Journal of Visualization, Vol. 4, No. 3 (2001) 285-298

An Algorithm for Evaluating Overlapping Bubble Images Recorded by Double Pulsed Laser Holography

Ohta, J.*[1], Mayinger, F.*[2], Feldmann, O.*[2] and Gebhard, P.*[2]

*1 Department of Mechanical Engineering, Fukui University, 3-9-1 Bunkyo, Fukui 910-8507, Japan.
*2 Lehrstuhl A für Thermodynamik, Technische Universität München, Boltzmanstraβe 15, Garching 85784, Germany.

Received 1 August 2000.
Revised 27 March 2001.

***Abstract*:** The present paper describes a method for evaluating images of a bubbly flow in stirred aerated tanks which are typical when pulsed laser holography is applied as the measuring technique. Features of the brightness histograms of reconstructed bubble images are discussed. A procedure is presented to evaluate the bubble images taken from a reconstructed hologram in order to determine the center of gravity of the bubble image. Double pulsed holograms were taken to measure bubble velocities and diameters simultaneously. In this case, overlapping bubble images are sometimes observed in the reconstruction. This significantly impedes the evaluation of the characteristics of the bubbles. Thus, an algorithm is presented in this work to distinguish between single and overlapping bubble images and to separate the overlapping bubble image in a two-dimensional image for a bubbly flow at low void fraction recorded from double pulse holograms. This algorithm was confirmed to be effective if the bubble images are extracted from the entire image.

***Keywords*:** image processing, overlapping bubble image, short time holography.

Nomenclature:

q	angle between two neighboring vectors (see Fig.10)
q_c	critical value for q_{min} (see Section 3.6)
q_{min}	local minimum of q-profile (see Section 3.4)
w_1	occurrence probabilities for the class that has lower values among three classes in the brightness histogram of a bubble image when the histogram is divided into three classes (see Section 3.3)
w_c	critical value for w_1 (see Section 3.6)
Dpixel	ratio of the pixel number of a vector to the total number of pixels for an outline of a bubble image (see Section 3.4)

1. Introduction

Knowledge of parameters such as the interfacial area of bubbles, bubble residence time, bubble distribution and power consumption is required to design an aerated stirred tank. To estimate these parameters theoretically, transport equations of mass, momentum and energy have to be solved. However, since disintegration and coalescence of bubbles usually occurs in the tank and the liquid phase is usually turbulent, which strongly affects bubble transport and bubble coalescence, these phenomena are not yet completely understood. Many efforts have been made to theoretically describe such phenomena in a bubbly flow, but many of these models have not yet been validated due to a significant lack of experimental data. Therefore, an experimental investigation of the two phase

flow in an aerated stirred tank was conducted at Technische Universität München. A broad set of experimental data on the bubble size distribution, the interfacial area and the bubble residence time in aerated stirred tanks has been generated. The short time holography has been applied as the measuring technique in these experiments.

Holographic Particle Imaging Velocimetry, or HPIV, was applied to a single-phase flow by Bahnhart et al. (1995) using a double pulsed laser. Their study employed a reference multiplexed, off-axis geometry to determine velocities using the cross-correlation technique. Mayinger and Chávez (1992) applied HPIV to measure the spray pattern and the condensation rate of saturated vapor onto a subcooled injection jet. The droplet diameter spectrum, droplet velocity distribution and the heat transfer coefficient were determined in these experiments. Mayinger and Gebhard (1995) extended the method by applying a biaxial optical setup for the recording, in which two holograms of the spray – perpendicularly to one another – were recorded simultaneously. Both recorded positions of each droplet were identified in one reconstructed image. The two-dimensional velocity vector was calculated by using these droplet positions. Three-dimensional droplet velocity vectors were then determined by applying a stereo matching algorithm to correlate the two recorded views. Mayinger et al. (1998) have applied this technique to a bubbly flow in an aerated stirred tank. However, the spray flow and the bubbly flow in a stirred tank differ significantly. The velocity and the size of the bubbles in a bubble column have a wider range of distribution compared to those of droplets in spray flow. In addition the flow of the bubbles in a stirred tank is not unidirectional. The images obtained from reconstructed double pulsed holograms sometimes showed two overlapping images of one bubble. These overlapping bubble images become a problem when an attempt is made to identify the bubble locations in order to measure their velocities. Sakaue and Takagi (1983), Song et al. (1998) and others proposed an algorithm for separating two or many more overlapping particle images. These studies regarded the shape of the particle images as circles so that the centers and the radii of the circles were estimated. The overlapping particle images were separated using these centers and radii. Since larger bubbles cannot be regarded as spheres, such algorithms are not suitable. Takahara and Etoh developed a particle mask correlation method (PMC method) in order to extract particle images whose shapes are circular or similar to circles (Takahara et al., 1997). They considered the particle mask as a template in pattern matching. They assumed the particle mask to have the shape of a two dimensional Gaussian distribution. The PMC method is powerful and can separate two adjacent particle images or overlapping particle images. However, it is difficult for the PMC method to separate overlapping particle images of various non-circular shapes. Obviously, some previous algorithms can be extended to an ellipse approximation using the parts of the outline of the overlapping particle images. However, the accuracy of ellipse fitting using the parts of the outline is very low (e.g. Ellis et al. 1992, Rosin, 1996).

In the present paper, the experimental setup used in the experiments performed at "Technische Universität München" is briefly explained. The presented images were obtained in the München test facility. This is followed by the introduction and a detailed explanation of an image processing algorithm which has been developed at Fukui University to evaluate overlapped bubble images. The development of this algorithm solves one of the biggest problems in determining the bubble's velocity distribution from double pulsed holograms: it separates the overlapping bubble images and determines the distance between their centers of gravity. In addition, criteria for classifying overlapping bubble images, and single bubble images, based on both the brightness histogram of the bubble image and the features of the outline of the full bubble image are presented. Although the proposed algorithm is developed for a bubbly flow at a low void fraction, it has the advantage of working successfully in the cases where bubble images cannot be approximated by an ellipse or circle. The presented algorithm is applicable also to bubble images whose outlines have slight concave parts or slight convex parts. Its structure, fields of application, and limitations will be discussed in the present paper.

2. Short-time Holography

Short-time holography is a non-invasive measuring technique highly suited to the analysis of transport phenomena (e.g. heat and mass transfer) in dispersed transparent flows. It records all light information scattered by or reflected on an object, both the amplitude and the phase distribution. The entire 3D optical information about the flow field in the test section is stored on the holographic plates. Particles with a diameter greater than ten times the wavelength of the laser light are imaged sharply. The principal features of this measuring technique are explained in more detail in the literature (Kiemle and Röss, 1969; Leith and Upatnieks, 1964; Mayinger, 1994; Mayinger et al., 1998). The following subsections describe the optical recording mechanism and the reconstruction apparatus as applied in the experiments at the Lehrstuhl A für Thermodynamik.

2.1 Experimental Setup

A rectangular vessel with a bottom area of 100 mm × 100 mm and a filling level of also 100 mm was applied as the bubble column. The vessel was made of glass, and distilled water was used as the liquid. The air was supplied into the vessel by means of a nozzle with a diameter of $d_N = 0.2$ mm which was located centrally in the flat bottom of the vessel. As the stirrer a Rushton-turbine with a diameter of $d_T = 40$ mm was applied. The distance between the bottom of the vessel and the stirrer was set to 50 mm.

2.2 Recording of the Holograms

Short-time holography is applied to the analysis of dispersion characteristics in an aerated stirred vessel. The optical setup is shown schematically in Fig. 1 (Feldmann, 1999). A pulsed ruby laser generates light pulses with a wavelength of $l = 694$ nm and an energy of $E = 1$ Joule for the exposure time of $t = 30$ ns. The emitted laser beam is collimated by passing through two lenses (CL) and is then split into two object beams and two reference beams by a bank of beam-splitters (BS). The object beams are diverted at the mirrors (M), are diffused by a ground glass plate (GG), then cross the test section perpendicular to one another. Upon exiting the test section, the object beams fall perpendicularly onto the holographic plates (H1, H2). The object beams contain the entire optical information of the test section. The reference beams are diverted directly to the holographic plates. The superposition of an object beam and a reference beam results in an interference figure which is stored on the coating of the holographic plates. The ruby laser can be operated either in a single pulse or double pulse mode. In double pulse mode, two successive holograms of the flow field in the vessel are stored on each holographic plate. With the knowledge of the pulse-separation and the evaluated holographic reconstruction, the velocity field of the bubbles can be determined. The pulse-separation of one laser can be varied from $Dt = 1$ ms to $Dt = 800$ ms.

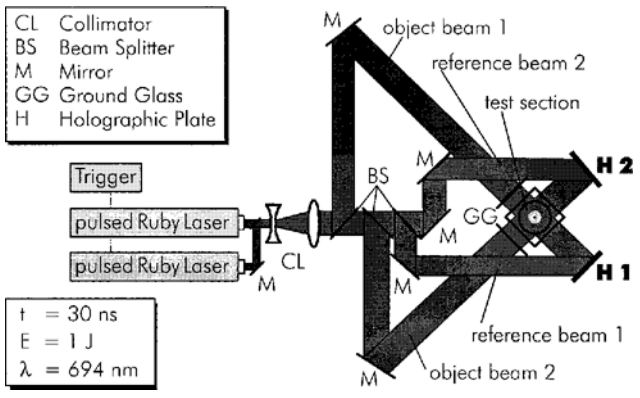

Fig. 1. Optical setup for recording.

2.3 Reconstruction and Evaluation of the Holograms

The developed plates – now called holograms – are reconstructed by illumination with a continuous HeNe laser beam. As a result, the object beam containing the entire optical information of the test section is reconstructed. In front of each holographic plate a stationary image, the real image of the recorded scene, is formed three-dimensionally and distortionless, as shown schematically in Fig. 2 (Feldmann, 1999). The spatial information of the entire measuring volume is furnished in three dimensions with a width of approximately $d = 120$ mm and an infinite depth of field. This 3D image is recorded by means of a CCD-camera. The camera lens has a large focal length and a small depth of field, so that only a small fraction of a reconstruction is in focus, as indicated by the gray bars in Fig. 3 (Feldmann, 1999). By moving the camera step by step along its depth coordinate, the entire 3D information contained in the holographic reconstruction is scanned and transformed into a series of 2D digital video images. The depth of field determines the step size and thus the resolution in the depth dimension. The images depicted in Fig. 3 reveal how the field of view of the camera changes with its position. Bubbles that are depicted sharply in one image are out of focus at a different camera position.

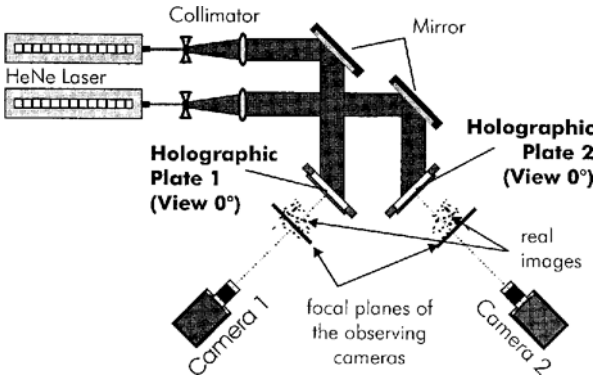

Fig. 2. Optical setup for reconstruction of image.

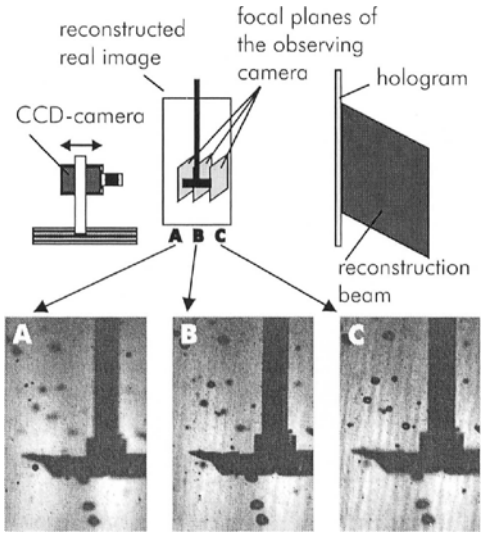

Fig. 3. Reconstructed images for three camera locations.

3. Image Processing

The images obtained by following the procedures described above were recorded at Technische Universität München. The main part of this work was done at Fukui University: the development of a sophisticated image processing algorithm to enable an automatic treatment of overlapping bubble images, which is one of the biggest problems appearing in hologram evaluation.

3.1 Brightness Histograms

(a) Single pulse

Examples of reconstructed bubbly flow images are presented along the depth coordinate of the entire 3D information in A, B and C of Fig. 3. Bubbles' images in the focus plane are seen clearly, however, bubbles' images in other regions are out of focus and blurred. Also, an example of a reconstructed image for single pulse is shown in Fig. 4. Overlapping bubble image can be seen in Fig. 4, since the bubbles locate close to each other. Brightness histogram of the overlapping bubble images for a single pulse is indicated in Fig. 6. There is one remarkable peak in the brightness histogram.

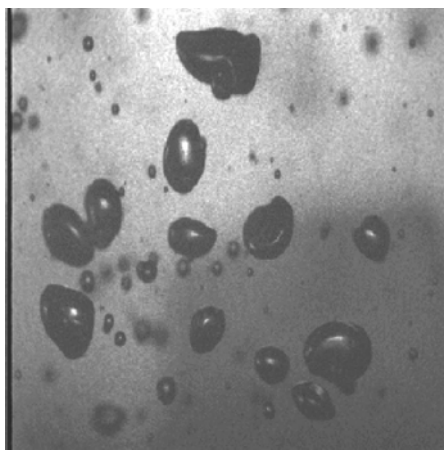

Fig. 4. Reconstructed image for a single pulse.

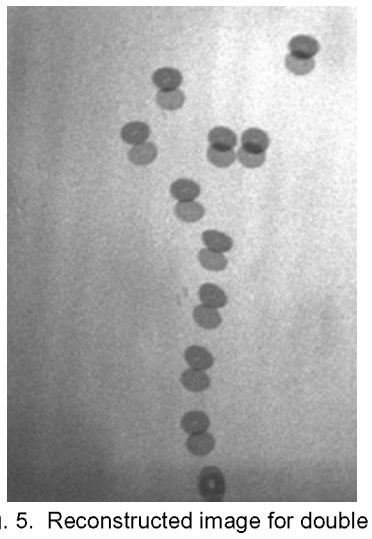

Fig. 5. Reconstructed image for double pulses.

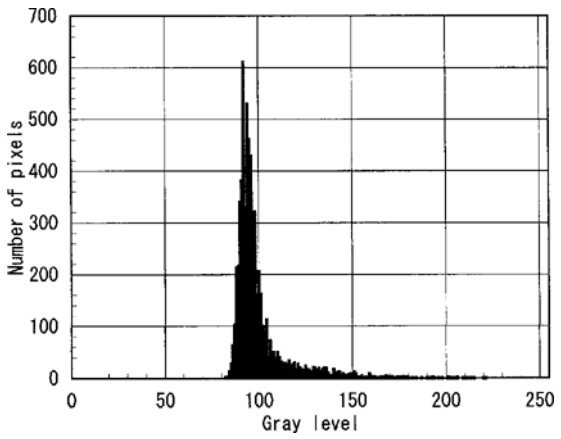

Fig. 6. Brightness histogram of overlapping bubble images for a single pulse.

(b) Double pulses

Examples of overlapping bubble images were shown in Fig. 5 for double pulses. The overlapping region is darker than all other bubble regions. Brightness histograms of bubble images are different depending on the overlapping area and the intensities of double pulsed laser. First, when the intensities for double pulsed laser are almost the same, examples of the brightness histograms of full bubble images are indicated in Figs. 7(a) and 7(b) for slightly overlapping case and for widely overlapping case, respectively. The brightness histograms of the full bubble images indicate one peak for the former and two peaks for the latter. Since the overlapping region is narrow in the former, sometimes the second peak cannot be clearly distinguished. Second, when brightness of one bubble image is slightly different from the other, an example of the brightness histogram of the full bubble image is shown in Fig. 7(c) for widely overlapping case. One peak includes two small peaks as shown in Fig. 7(c), in other words two higher frequency waves are superimposed on one peak, corresponding to the small brightness difference between the two bubble images. Probably, many factors, such as difference between the first and second laser pulse intensities, spatial intensity distribution of laser beam, i.e. background gray level distribution and so on, are considered to cause the brightness difference. From Figs. 7(a), (b) and (c), more than two peaks are seen in the overlapping bubble image for double flashes. On the other hand, one peak is observed both in the bubble image for single flash and in the slightly overlapping bubble image for double flashes.

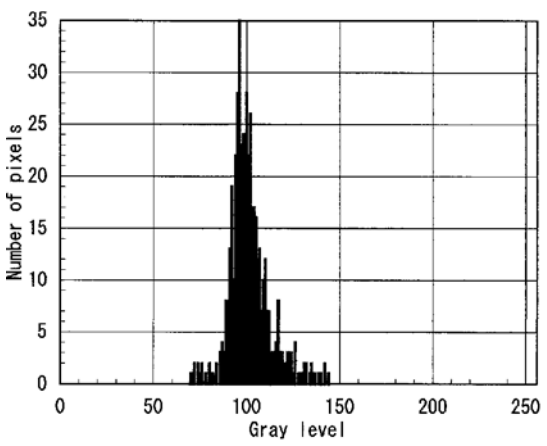

(a) slightly overlapping.

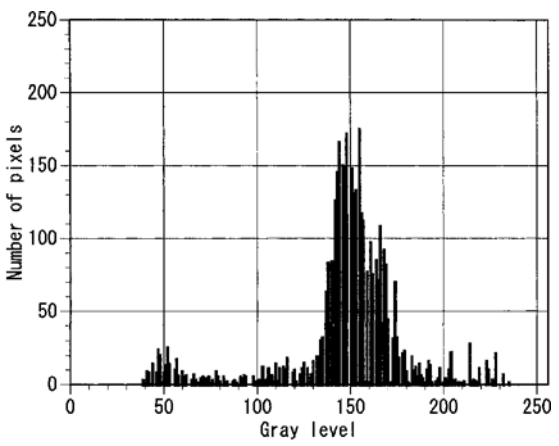

(b) two bubbles brightness is the same.

Fig. 7. (Continued).

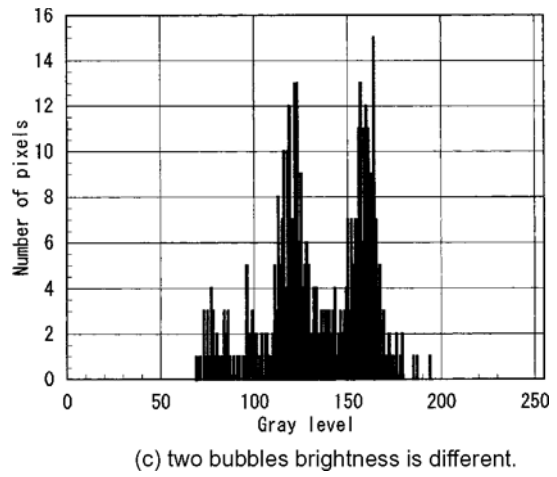

Fig. 7. Brightness histogram of an overlapping bubble image for double pulsed laser holography

3.2 Procedure

A sketch of an overlapping bubble image of one bubble is drawn for double pulsed laser holography in Fig. 8(a). Roughly speaking, the overlapping bubble image looks darker in the overlapping region and brighter in the other regions. Thus, when the brightness histogram of the bubble image has more than two peaks, it can be assumed that the bubbles in the image overlap. However, when the brightness histogram of the bubble image has one peak, it cannot be always assumed that the bubble in the image does not overlap, as mentioned Section 3.1. Thus, it is not sufficient to distinguish between overlapping and non-overlapping bubble images based strictly on the number of peaks in the brightness histogram of the full bubble image. Therefore, a new algorithm is proposed for treating overlapping bubble and single bubble images for double pulsed laser holography. A flowchart of the proposed algorithm is shown in Fig. 9. The proposed algorithm distinguishes between overlapping and non-overlapping bubble images, separates the overlapping bubble images, and measures the centers of gravity of the bubbles. These procedures are explained as follows:

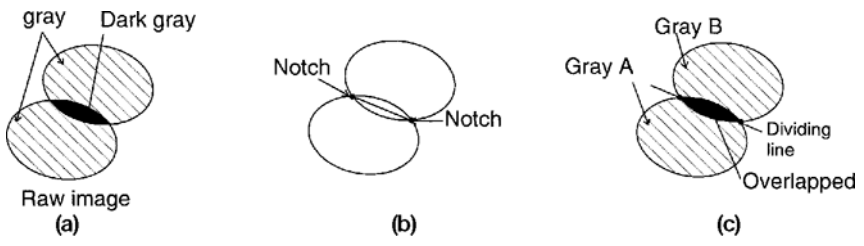

Fig. 8. Dividing line and gray regions.

(a) Map for mask regions corresponding to bubble image

First, a map of the mask region for bubble images is obtained so that the bubble images can be treated individually (see the upper part in Fig. 9). The outlines of the bubble images are extracted from an original full frame image by an edge detection technique using commercial software. Thick and complicated outlines of the bubble images and various noises remain in the full frame image after edge detection. Blurred bubble images and the other noises are removed from the full frame image. Then, the treated full frame image is transformed into a binary-image. All pixels representing the outlines of the bubble images are detected in the full frame image. Next, the region inside the bubble outline is filled in. This filled region is defined as the mask region of the bubble image. A bubble number ("iobje" in Fig. 9) is registered for all of the pixels that are located inside the mask region.

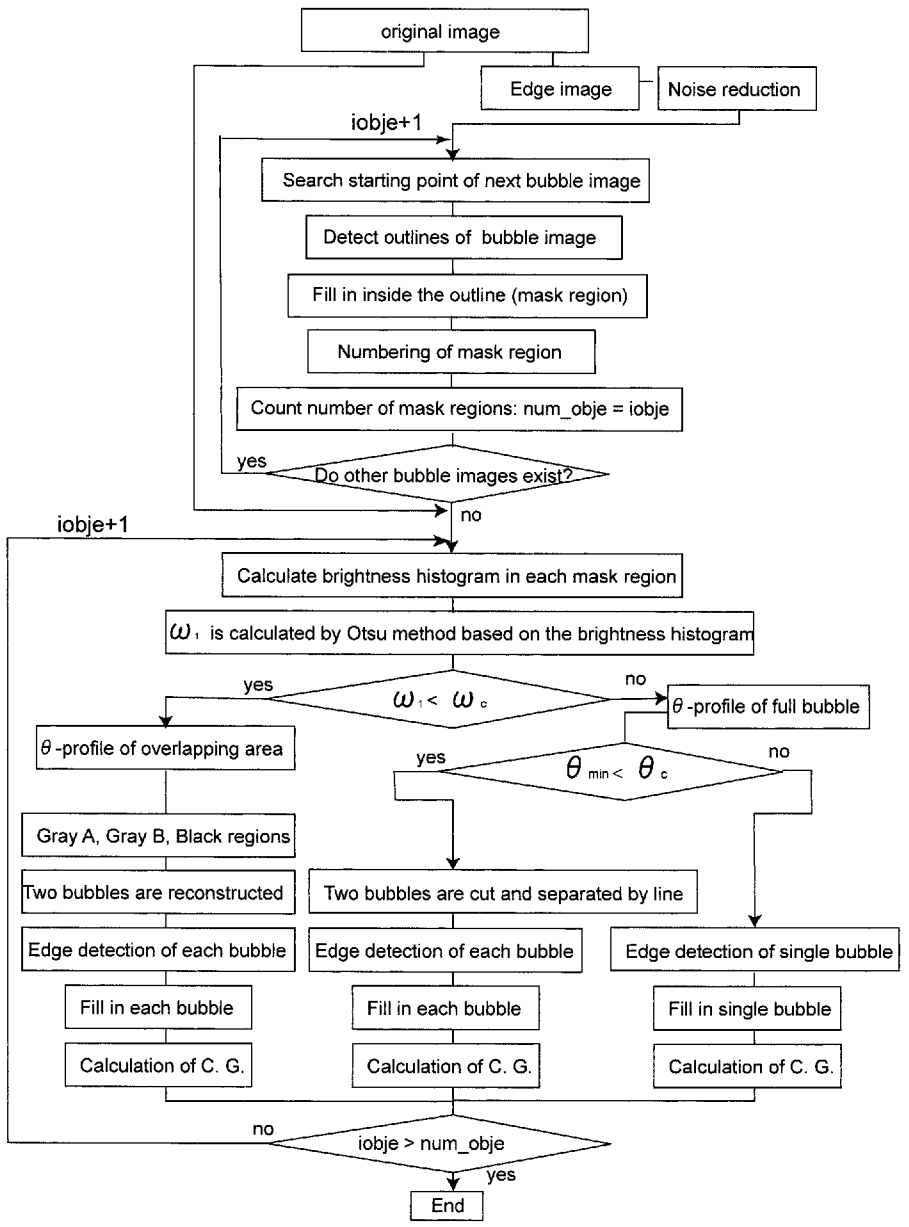

Fig. 9. Flowchart of the proposed algorithm.

(b) Classification of bubble image using W_1 *and* q_{min}

In the present paper, each of the original bubble images is classified as being either an overlapping bubble image, a contacting bubbles image or a single bubble image based on the values of W_1 and q_{min} (see the lower part in Fig. 9). The variables of W_1 and q_{min} are explained briefly.

A brightness histogram is obtained from a gray bubble image within the mask region. The brightness histogram of the bubble image is statistically separated into three classes in order of brightness level, i.e. Class 1, Class 2 and Class 3, by Otsu method, which will be described in Section 3.3. The brightness levels (8 bits) of 1 and 256 correspond to black and white, respectively. Occurrence probabilities of Class 1, Class 2 and Class 3 are denoted as W_1, W_2 and W_3, respectively. The value W_1 of a given bubble image is found to be a useful parameter for classifying the arrangement of the bubble image in the present study.

The features of the outline of the full bubble image must correspond to the arrangement of the bubble image. The term of q_{min} is the local minimum angle between two vectors of the outline of the full bubble image. It will be explained in Section 3.4 in details.

Criteria of this classification are explained as follows:

Case A: If the value of W_1 for a given bubble image is less than that of W_c, which is a critical value of W_1, the bubble image can be regarded as an overlapping bubble image. Thus, the overlapping bubble image is separated by the method explained in Section 3.5 (a).

Case B: If the value of W_1 is greater than that of W_c, and the values of the first- and second-lowest q_{min} are less than that of q_c in the "q- profile", the bubble image can be judged to be a contacting bubbles image or a slightly overlapping bubble image. q_c is a critical value of q_{min}. Such bubble images are separated by the method described in Section 3.5 (b).

Case C: If the value of W_1 is greater than that of W_c, and the value of q_{min} is greater than that of q_c, the bubble image can be assumed to be a single bubble image†. Therefore, it is not necessary for the image to be separated.

Case D: If there is only one local minimum in the "q-profile," the bubble image is regarded as a single bubble image, even if W_1 is less than W_c. This case sometimes occurs in bubble images that consist of less than about 30 pixels.

Case E: The value of W_1 is less than that of W_c, and the value of q_{min} is greater than that of q_c. In this case, judgment is impossible.

This procedure (shown in the lower part of the flowchart in Fig. 9) is repeated, until the bubble number "iobje" reaches to the number of the bubble images "num_obje". After this process is completed, single bubble and separated bubble images are obtained, the centers of gravity of which are calculated by the moment method.

3.3 Calculation of W_1

The method of obtaining W_1 and threshold value k_1 for separating an overlapping bubble image is explained in this section. Otsu method (Otsu, 1979) was originally developed in order to extract clear object images from a full frame gray scale image by classifying the brightness histogram of the full frame image into two or more classes. Since bubble images are recorded using double pulsed laser and the intensities for the two lasers are not always equal, in the present paper it is assumed that the brightness histogram of one bubble image can be divided into three classes: S_1, S_2 and S_3. These three classes are expressed using threshold values k_1 and k_2 as $S_1 = (1, 2, ..., k_1)$, $S_2 = (k_1 + 1, ..., k_2)$ and $S_3 = (k_2 + 1, ..., k_3)$. Where the numbers in parentheses represents the brightness level of the histogram, and k_3 is 256.

$$V(k) = \sum_{i=1}^{k} p_i, \qquad m(k) = \sum_{i=1}^{k} i p_i$$

where p_i is the normalized histogram for a given brightness level i of the bubble image; $W(k)$ is probability distribution function of an extent of brightness levels, $m(k)$ is the first-order moment, and $m(256) = m_T$. Probability distribution functions for classes S_1, S_2 and S_3 are calculated from the brightness histogram of a bubble image, and are expressed by W_1, W_2 and W_3, respectively.

$$V_1 = \sum_{i \in S_1} p_i, \qquad V_2 = \sum_{i \in S_2} p_i, \qquad V_3 = \sum_{i \in S_3} p_i$$

Using these variables, S_B^2 is defined by

$$S_B^2(k) = V_1 \left(\frac{m(k_1) - m(1)}{V(k_1) - V(1)} \right)^2 + V_2 \left(\frac{m(k_2) - m(k_1)}{V(k_2) - V(k_1)} \right)^2 + V_3 \left(\frac{m(k_3) - m(k_2)}{V(k_3) - V(k_2)} \right)^2 - m_T^2$$

where $k_1 < k_2 < k_3 = 256$. The combination of k_1 and k_2 that gives the maximum S_B^2 is taken as the appropriate threshold values for the brightness histogram of the bubble image that is to be divided into three classes.

---

† Since laser pulse duration is chosen not to record fully overlapping bubbles image or bubbles image for which the overlapping area is more than about 50% of the single bubble area, a single bubble image does not need to be considered as a fully overlapping bubble image. Even if a bubble moves in the optical depth direction during laser pulses, the bubble image can be taken as a single bubble in the reconstructed plane. It is difficult to distinguish between the patterns of single bubble image and fully overlapping bubble image by only referring the brightness histogram of the bubble image from one view. Measuring the bubble velocity components in the reconstructed plane is difficult when the overlapping area of the bubble image is more than about 50% of the single bubble one.

3.4 Finding Notches of the Outline of the Bubble Image: q_{min}

The present paper uses the angle between two neighboring vectors on the outline of an extracted bubble image (see Fig. 10). In order to construct two neighboring vectors three consecutive points are taken on the outline pixels and are labeled points A, B and C in that order. Constant number of pixels is assigned to the vectors BA and BC. The angle q between vectors BA and BC is calculated. The ratio of the constant number of pixels to the total number of pixels for the outline of a bubble image is denoted as "Dpixel" in the present paper. We can now obtain the profile of q against the pixel number of the point B (q vs. pixel number). q is filtered three times by the five adjacent q_s using the F-operation (Eccles et al., 1977). In the present study, the filtered q-profile is called as "q-profile". When the first- and second-lowest local minimums (q_{min}) are found in a "q-profile" of the full bubble image, the two locations correspond to the two notches of the outline of the full bubble image. Two methods can be used to find the notches of an outline in an overlapping bubble image. One method involves finding the notches of the outline of the full bubble region, and the other method involves searching for the sharp part in the outline of the overlapping area. In the method for the outline of the overlapping area, the procedures are almost identical to those presented above, but the first- and second-highest maximums q are used instead of q_{min}.

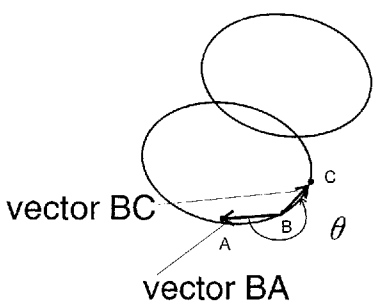

Fig. 10. Angle between two neighboring vectors.

3.5 Method for Separating Overlapping Bubble Images

(a) Overlapping bubble image

The threshold value k_1 between S_1 (Class 1) and S_2 (Class 2) for the brightness histogram of the bubble image is obtained by Otsu method (1979). The overlapping area is extracted from the full bubble image using the threshold value k_1. The line that passes through the two notches of the outline is determined (see Fig. 8(b)). In the present paper, this line is referred as dividing line. Pixels in the full bubble region are divided into gray A, gray B and overlapping regions using the dividing line (see Fig. 8(c)). One bubble image is reproduced from the gray A and overlapping regions, and the other bubble image is reproduced from the gray B and overlapping regions.

(b) Contacting bubbles image or slightly overlapping bubble image

For a contacting bubbles image or a slightly overlapping bubble image, the procedure for obtaining the outline of the full bubble image can be used. The q-profile of the entire outline of the full bubble image is calculated. The first- and second-lowest local minimums are searched in the q-profile. Then, the dividing line is obtained in the manner described above. Since the overlapping region in the full bubble image is narrow, each bubble region can be separated using the dividing line.

3.6 Critical Values of w_c and q_c

The value of w_c is chosen to range from 0.32 to 0.35 for bubble images having an overlapping area of less than about 50% for double pulses in order to distinguish between overlapping and single bubble images. This reason is as follows.

In the case of the Gaussian brightness level distribution, the values of probability distribution functions w_1, w_2, and w_3 are calculated by Otsu method, to be 0.28, 0.44 and 0.28, respectively. The brightness histogram of a single bubble image is considered to be similar to the Gaussian distribution. However, the shape of the brightness histogram of a single bubble image tends to differ from the Gaussian and to be similar to the histogram in Fig. 6. Hence, the value of w_1 of a single bubble image is greater than that of the Gaussian distribution. From many bubble images, the value of w_1 is greater than 0.4 for a single bubble image. In the case of contacting bubbles images, the values of w_1 are 0.36 to 0.6 empirically. Moreover, if more than 60% of a single bubble image area is

overlapping, it becomes very difficult to find local minimums in the q-profile correctly. Therefore, bubble images that have an overlapping area of more than 60% are not usually treated in the present algorithm.

The value of q_c is chosen to be between 180° and 190°. Since the q-profile is filtered using the F-operation, q_{min} becomes higher than the real angle between the two vectors.

3.7 Other Effects

After smoothing is performed on the original brightness histogram of the bubble image, the relative change of W_1 value is less than 10%. Thus, a one-time smoothing operation does not influence the judgement. When number of pixels that constitute a bubble image is less than 20 to 30, the value of W_1 is not always greater than 0.35 for a single bubble image. This algorithm depends on statistics in order to obtain the value of W_1. If the number of pixels that constitute the bubble image is too low, the effect of scattering of the brightness values in the small bubble image on the calculation of W_1 is not always negligible.

A brighter spot area in a bubble image, as in Fig. 5, may affect the values of W_3 and k_2 directly. This is because the brightness level of the brighter spot area belongs to Class 3, i.e. S_3. Therefore, the value of k_1 is not affected by the brighter spot area. It may slightly affect the value of W_1, because $W_1 + W_2 + W_3 = 1$. However, the brighter spot area in a bubble image does not affect the present algorithm from the point of view of W_c. The reasons are as follows: Firstly, the diameter of the brighter spot is less than that of the corresponding bubble. Secondary, the empirical critical value of W_c is determined from many bubble images, including images containing brighter spot area. Before calculating the center of gravity of the bubble image, the brighter spot area in the bubble image is filled in. Thus, the brighter spot area does not influence the calculation of the C.G. of the bubble image.

3.8 Limitations of the Algorithm

Since this algorithm utilizes brightness histograms of bubble images, the algorithm can be applied to overlapping bubble images due to double flashes. The bubble outlines in the image must be completely visible, because the algorithm uses the outlines of the bubble images. This algorithm cannot be assumed to classify the bubble image correctly when the overlapping area is greater than approximately 50% of the single bubble images, as mentioned in Section 3.6, or when the overlapping bubble image consists of less than about 100 pixels, as described in Section 3.7. When the bubble concentration is higher, several images of the bubbles are expected to overlap each other. For the proposed algorithm to be effective, the outline of a bubble image must not be blurred by other bubbles that are out of focus.

4. Results and Discussions

4.1 Brightness Histogram of Bubble Image and W_1

Examples of bubble images are shown in the upper part of Figs. 11(a), (b), (c) and (d). These images were extracted from a wider field image. Image (a) was recorded at a stirrer rotational speed of 250 rpm, and the time delay for the two lasers was 4 ms. Images (b), (c) and (d) were recorded at a stirrer rotational speed of 500 rpm, and the time delay for the two lasers was 5 ms. The calculated values of W_1 are 0.092, 0.077, 0.154 and 0.425 for images (a), (b), (c) and (d), respectively. The value of W_1 for image (d) is greater than W_c. This will be discussed in Section 4.3.

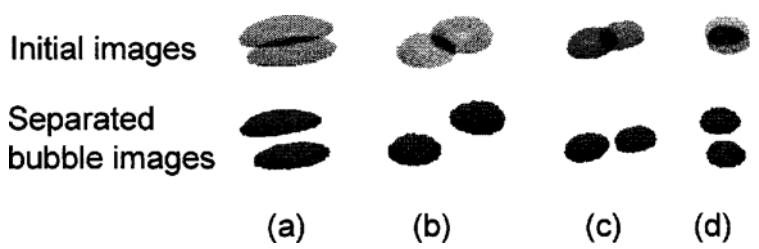

Fig. 11. Initial bubble images and separated bubble images.

4.2 Angle between Neighboring Vectors: q-profile

q-profiles for the full bubble outlines of images (a), (b), (c) and (d) are presented in Fig. 12. By trial and error, a *D*pixel of around 8% was found to be appropriate for finding local minimums in the case of the full bubble outline in many images. The local minimums are indicated with vertical arrows in the figure. The pixel numbers at the local minimums match those at the notch of the full bubble outline for images (a), (b) and (c). However, the two local minimums of image (d) indicated by vertical arrows and marked "wrong" reveal that the local minimums do not match the notches in the outline of the full bubble image. This is because the two bubbles of image (d) have a greater overlapping area, thus the first- and second-lowest local minimums do not correspond to the correct notches of the outline of the full bubble image.

After examination, a *D*pixel of around 10% was found to be suitable for finding local maximum values for the outline of the overlapping area of the bubble image. *q*-profiles of the outlines for overlapping area images (a), (b), (c) and (d) are shown at a *D*pixel of 10% in Fig. 13. The local maximums are indicated by vertical arrows in Fig. 13. From this figure, two local maximums are easily identified in each *q*-profile. The two local maximums are confirmed to correspond to the sharp angle of the outline.

If an overlapping bubble image is extracted completely, i.e. no part of the bubble outline is missing, the notch locations are more easily obtained in the outline of the overlapping area image than in the outline of full bubble image. When two bubble images have a greater overlapping area, the method for separating the bubble image that uses the outline of the overlapping area is more accurate than that which uses the outline of full bubble images. However, since local minimums of the *q*-profile for the full bubble image are always used to distinguish

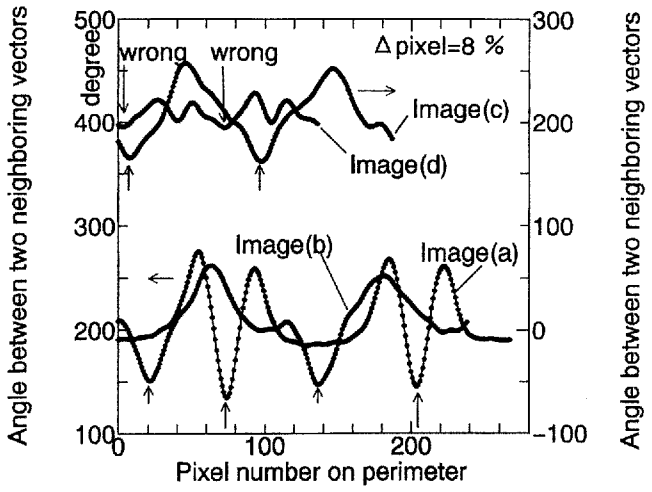

Fig. 12. *q*-profiles of outlines for a full bubble region.

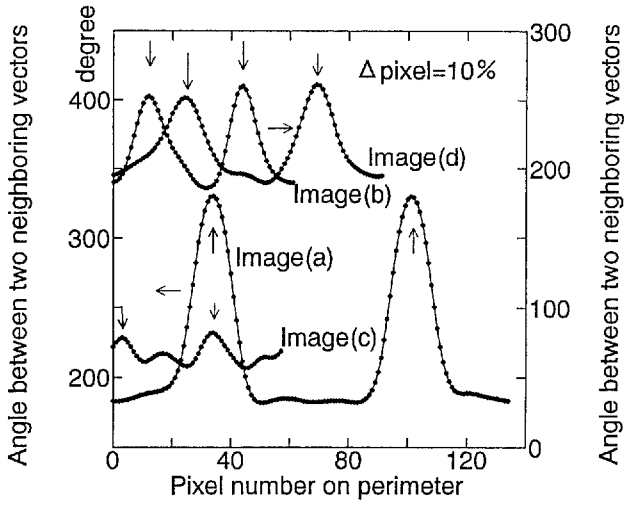

Fig. 13 *q*-profiles of outlines for an overlapping region.

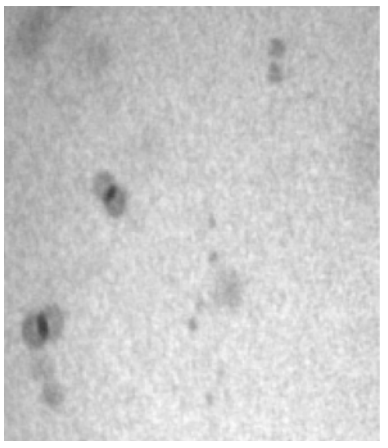

Fig. 14 Reconstructed bubble images in a stirred tank.

between overlapping and non-overlapping bubble images, as explained in Section 3.2(b), using the outline of the full bubble image is convenient.

4.3 Bubbles Images

Initial images were shown in the upper part of Figs. 11(a), (b), (c) and (d). The bubble images are separated from the initial images using the proposed algorithm and are presented in the lower part of Fig. 11. The overlapping bubble images are separated and drawn as individual bubbles in the figure. However, if the value W_c is assumed to be 0.35, image (d) is not judged to be an overlapping bubble image. This is attributed to the fact that the bubble in image (d) has an overlapping area that is more than 50% of the single bubble area. Thus, the value of W_c is chosen as 0.45 for image (d) only. Image (d) is an exception to which the proposed algorithm cannot be applied directly. The bubble images are separated correctly. Thus, when a bubble image is extracted completely from the whole field and it has overlapping area less than 50% of the single bubble area, the proposed algorithm can be used to separate the overlapping bubble image produced by double pulsed laser holography and the two centers of gravity of the bubble image can be obtained. The measured 2-D velocities are 0.38, 0.83, 0.41 and 0.13 m/s for the images of (a), (b), (c) and (d), respectively. Compared with the terminal rising velocity, the value of 0.83 m/s is higher. The bubble in image (b) was located close to the stirrer, so that the stirrer's rotational movement caused the bubble to achieve a high velocity.

Figure 14 shows the original reconstructed image of bubbles in the tank for double pulses. The edge image was extracted from the original image by means of a commercial program. The present algorithm processed the original image and binary edge image. As a result, it judged that one pair of bubble images in the upper right part of the image region represented single bubbles and that the two pairs of bubble images in the lower left part of the original image were overlapping ones. As seen from Fig. 14, this result obtained by the present algorithm can be considered to be reasonable. The overlapping bubble images were separated by the present algorithm. The measured equivalent diameters and 2-D velocities of the upper overlapping bubble and the lower overlapping bubble images were 0.95 mm, 0.124 m/s and 1.08 mm, 0.127 m/s, respectively. Since all other bubble images in the figure were recognized as out of focus ones by either way of processing the original image into the binary edge image or by way of noise reduction, these other bubble images were all deleted.

4.4 Comparison with the Manual Method

Software for obtaining and modifying photo images is readily available. Thus, an overlapping bubble image is fed into a personal computer, and each bubble image is extracted by a process of trial and error from the overlapping bubble image using commercial software (Corel DRAW 5). Next the C.G.s of the bubble images are calculated by the moment method for each image. This method is called the manual method in the present paper. The x and y coordinates of the C.G.s for the images using the double pulsed laser holography are obtained by the present algorithm and the manual method, respectively. The latter results may contain some errors. However, these C.G.s appear to be correct within visible when viewed by the naked eye. Deviation of measured data from that of the manual method is estimated using the standard error of estimation (ASME, 1985), or SEE. The errors were 0.47

pixels and 0.45 pixels for the x and y directions, respectively. The present results are in good agreement with the results obtained by the manual method. Thus, the present algorithm is confirmed to work two-dimensionally for an overlapping bubble image, as long as the bubble image is extracted, without missing part of the bubble image.

5. Concluding Remarks

When double pulsed laser holography is applied to determine bubble velocities and diameters in an aerated stirred vessel, overlapping bubble images are sometimes observed in the reconstructed images. This work presented (a) criteria to classify overlapping bubble images, contacting bubbles images and single bubble images, based on both the brightness histogram of the full bubble image and the features of the outline of the full bubble image and (b) a procedure to separate the features of overlapping bubble images.

The relationship between the bubble arrangements in the images for single pulse and double pulsed laser holography and W_1 (statistical value) of the brightness histogram of the bubble images was discussed.

Bubble images were classified as being an overlapping bubble image, a contacting bubbles image or a single bubble image, based on the values of W_1 and $q_{\min}$ for the outline of the full bubble image.

An algorithm was proposed for classifying the bubble images and separating the overlapping bubble images into individual bubble images, thereby enabling the center of gravity of each bubble image to be obtained. The proposed algorithm was confirmed to work in two-dimensional image, as long as the bubble image was extracted from the original full frame image without missing part of the bubble image.

The proposed algorithm is not applicable when the bubble outlines in the image are not visible completely. In addition, the proposed algorithm cannot always classify the bubble image correctly in the case of an overlapping bubble image that consists of less than about 100 pixels or that has an overlapping area that is greater than approximately 50% of the single bubble image area. When the bubble concentration is higher, the images of several bubbles are expected to overlap each other. However, for the algorithm to be effective, the outline of the bubble image must not be blurred by other bubbles that are out of focus.

Acknowledgment

The proposed algorithm was developed during the first author's stay in Technische Universität München under the support of Humboldt Foundation. The first author wishes to express his gratitude to the Foundation and his acknowledgement to Prof. Dr. Fujio Yamamoto, Fukui University, for his encouragement. In addition, the authors would like to extend their thanks to Dipl.-Ing. Robert Tauscher for his advice and to Dipl.-Ing. Sven Eisen for introducing software. The authors would also like to express their thanks to the reviewers for their careful review and good suggestions.

References

ASME, Measurement Uncertainty, ANSI/ASME Performance Test Codes 19.1, (1985).

Bahnhart, D. H., Adrian, R. J. and Papen, G. C., Recent Results of a Phase-conjugate Holographic System for High Resolutions Particle Image Velocimetry, Proc. SPIE 2333, (1995), 321-332.

Corel DRAW5, Corel Corporation Ltd., Harcourt Street Doublin, 2, Ireland

Eccles, M. J., Mcqueen, M. P. C. and Rosen, D., Analysis of the Digitized Boundaries of Planar Objects, Pattern Recognition, 9 (1977), 31-41.

Ellis, T, Abbood, A. and Brillault, B., Ellipse Detection and Matching with Uncertainty, Image and Vision Computing, 10-5 (1992), 271-276.

Feldmann, O., Short Time Holography and Holographic PIV Applied to Engineering Problems, Applied Optical Measurements, Springer-Verlag, Heiderberg, (1999), 263-278.

Freeman, H., On the Digital Computer Classification of Geometric Line Patterns, Proc. Natl. Elect. Conf. 18 (1962), 312-324.

Kiemle, D. and Röss, A., Einführung in die Technik der Holographie, (1969), Akademische Verlagsgesellschaft, Frankfurt, Germany.

Leith, E. N. and Upatnieks, J., Wavefront Reconstruction with Diffused Illumination and Three Dimensional Objects, J. Opt. Soc. of America, 54-11 (1964), 1195-1301.

Mayinger, F., Optical Measurements, Techniques and Applications, (1994) Springer-Verlag, Berlin, Germany.

Mayinger, F. and Chávez, A., Measurement Direct-contact Condensation of Pure Saturated Vapor on an Injection Spray by Applying Pulsed Laser Holography, Int. J. Heat Mass Transfer, 35-3 (1992), 691-702.

Mayinger, F. and Gebhard, P., Evaluation of Pulsed Laser Holograms of Flashing Sprays by Digital Image Processing, ASME FED-Vol.209, Flow Visualization and Image Processing of Multiphase Flow, (1995), 13-22.

Mayinger, F., Feldmann, O. and Gebhard, P., Evaluation of Pulsed Laser Holograms of Flashing Sprays by Digital Image Processing and Holographic Particle Image Velocimetry, Nuclear Engineering and Design, 184, (1998), 239-252.

Otsu, N., A Threshold Selection Method from Gray-level Histogram, IEEE Trans. System, Man and Cybernetics, SMC 9-1 (1979), 62-66.

Rosin, P. L., Assessing Error of Fit Functions for Ellipses, Graphical Models and Image Processing, 58-5 (1996), 494-502.

Sakaue, K. and Takagi, M., Separation of Overlapping Particles by Iterative Methods, Johoshori Gakkai Ronbunshu, 24-5 (1983), 561-567. (in Japanese)

Song, X., Yamamoto, F., Iguchi, M., Shen, L., Ruan, X. and Ishii, M., A Method for Measuring Particle Size in Overlapped Particle Images, ISIJ International, 38 (1998), 971-976.

Takahara, K., Etoh, T., Michioku, K. and Kuno, S., A Study on Particle Identification in Particle Mask Correlation Method, Proc. 2nd International Workshop on PIV '97 (Fukui), (1997), 213-220.

Author Profile

Junichi Ohta: He got his Doctor degree in Mechanical Engineering in 1984 from the graduate school of Engineering, Hokkaido University, Japan. He studied as research associate at Kobe University, Japan. Since 1992, he has been associate professor at Fukui University in Japan. His research interests are multi-phase flow, flow visualization and energy conversion.

Franz X. Mayinger: He got his degree (Dipl.-Ing.) in Mechanical Engineering in 1955. In 1961 he obtained his Ph.D. (Dr.-Ing.) in the field of thermodynamics from the Technische Universität München. Having worked in the industry for seven years he then became Professor and Director of the Institut für Verfahrenstechnik of the Universität Hannover in 1969. Since 1981 he has been owner and Professor of the Lehrstuhl A für Thermodynamik of the Technische Universität München. His main research incorporates the field of multi-phase flow, safety of nuclear power plants, heat transfer and the thermodynamic analysis of combustion processes as well as the development and application of optical measurement techniques. His research has been documented in five books and more than 280 publications. Additionally, he has been member of the reactor safety committee of the German Government, the scientific advisory board of the Bavarian government, as well as of international scientific organizations, such as the International Centre of Heat and Mass Transfer. He has been editor of several international journals, e.g. Heat and Mass Transfer. He obtained the Max Jacob Award (1991) for his merits in the field of optical measurement techniques and a honorary doctor (Dr.-Ing. E.h.) from the Universität Hannover in 1994.

Oliver Feldmann: He got his degree (Dipl.-Ing.) in Mechanical Engineering from the Technische Universität München, Germany, in 1996. He currently works on the determination of the bubble-sizes, the bubble-velocities, and the fluid dynamics of the continuous phase in aerated, stirred vessels at the Lehrstuhl A für Thermodynamik of the Technisch Universität München, Germany.

Peter Gebhard: He got his degree (Dipl.-Ing.) in Mechanical Engineering in 1991. In 1996 he obtained his Ph.D. (Dr.-Ing.) degree at Technische Universität München, Germany. His research interests are mainly in the field of analyzing flashing sprays and in describing the mechanisms of the spray-disintegration-process. He developed a Holographic Particle Imaging Velocimetry (HPIV) in order to determine both, the sizes and the velocities of the generated droplets. He currently works in the research department of AUDI.